To appear in the Proceedings of the 1999 IEEE
International Conference on Robotics & Automation
Detroit, Michigan · May 1999

Fluorescent Dye Based Optical Position Sensing for Planar Linear Motors

Gregory A. Fries, Alfred A. Rizzi, and Ralph L. Hollis
The Robotics Institute, Carnegie Mellon University
{fries+, arizzi+, rhollis+}@ri.cmu.edu

Abstract

Industrial Sawyer motor technology has existed for nearly three decades, traditionally being operated as open-loop positioners. Such systems can attain micron level motion resolution and open-loop repeatability of 10 μm. This paper outlines a optical sensing technique for Sawyer motors which is capable of sub-micron resolution. Such a sensor can easily be integrated into a motor enabling closed-loop control and sub-micron repeatability.

1 Introduction

Sawyer motors are a class of two-degree-of-freedom stepper motors which operate in the plane. The Sawyer motor, see Fig. 1, is composed of a forcer and stator side, with the forcer being the active or moving element. The stator is formed by a passive steel surface with orthogonally machined grooves, resulting in a waffle-iron-like pattern. These grooves are then filled with an epoxy in order to support an air bearing, upon which the forcer floats. The forcer is composed of two pairs of motor sections oriented orthogonally and capable of generating force in each of the principal directions as well as a torque. Each of these sections is made up of a permanent magnet and two drive coils. Energizing these coils produces force by directing the flux generated by the permanent magnetic to two sets of poles [1].

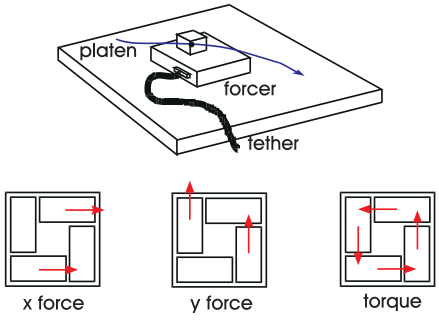

Figure 1: Representation of Sawyer motor unit.

A significant advantage of this configuration is that the workspace of the device is only limited by the size of the stator, or *platen*, while the precision is dictated by the ability of the forcer to micro-step. Current commercial Sawyer motors operating as open-loop positioners and can typically deliver resolution of 2 μm and repeatability of 10 μm, but are unable to reject external disturbances.

This paper presents a new type of optical sensor which is capable of sensing micron level motions of the forcer. Such a sensor provides the ability to sense relative motions at a resolution equal to that of the forcer's motion capabilities. By integrating this sensor with a commercial motor the repeatability of the complete system can be brought to 1 μm. Furthermore, a fast and accurate sensor enables closed-loop control of the forcer, allowing for decreased settling times and reduced energy consumption.

In the Microdynamic Systems Laboratory[1] at Carnegie Mellon University we are integrating Sawyer motor technology into the new concept of a modular *minifactory* [2]. One application for minifactory is the assembly of precision electro-mechanical devices. A major challenge in assembling these devices is achieving the increasingly tight tolerances, demanded by continuing product miniaturization. Minifactory offers a flexible, modular system capable of achieving these tolerances while affording rapid factory setup and reconfiguration.

2 Background

A sensor which enables a Sawyer motor to operate in a closed-loop fashion must provide accurate relative displacements at a high bandwidth. Previous attempts at creating sensors have used capacitive [3], magnetic [4, 5], and optical [6, 7] techniques. Of these, the magnetic technique has been the most thoroughly investigated, and our laboratory has produced a sensor with sub-micron resolution and a 14 kHz sampling rate [5]. Experiments with this sensor integrated into a commercial motor have shown that such a system is capable of sub-micron repeatability, improved tracking,

[1] http://www.cs.cmu.edu/~msl

and decreased settling time relative to open-loop motor operation [8].

We have continued the research project outlined in [7] by exploring an optical technique which is completely decoupled from any magnetic influences of the forcer. Every optical technique presumes that it is possible to optically sense the presence of platen teeth (high points in the waffle-iron pattern which are not coated by epoxy). One particular method of optically sensing these teeth is achieved by using a light sensitive component which "looks" through an interpolating mask. As the sensor moves orthogonally to the grooves of the mask, returned light energy from a source will have a "sawtooth" modulation of the form

$$E_s(x) = \begin{cases} E_{max}\left(\frac{1}{2} + \frac{x}{\tau}\right) & 0 \le x \le \frac{\tau}{2} \\ E_{max}\left(\frac{3}{2} - \frac{x}{\tau}\right) & \frac{\tau}{2} \le x \le \tau. \end{cases} \quad (1)$$

Here, x represents the displacement of the device in a direction orthogonal to the slits in the mask and τ is the pitch of the platen.

The correspondence of the peaks in the "sawtooth" to the geometry of the platen depends on the particular sensing technology used. For a sensor which measures reflected light, the maximum returned energy might occur when the pattern within each slit is composed of the tooth tops and epoxy. In a sensor which measures light re-emitted from the epoxy, as the one outlined in this paper does, the maximum signal occurs when the slit is aligned with the epoxy-filled grooves.

The only other evidence of an existing optical sensor appeared the first quarter of 1998 when Yaskawa, Inc. reported to release an optical sensor with similar performance. This sensor uses a new proprietary technique and no information has been released regarding its nature.

3 Optical Design Characteristics

The sensor described here measures light emitted from a laser dye that is mixed with the epoxy and is excited by a light source. In order to obtain the proper sensor characteristics a functional light source, filter and dye combination were selected. One limiting constraint is that all commercially available laser dyes, which do not denature in epoxy, have an absorption spectrum in the visible blue to ultraviolet range. Yet another constraint is that the entire sensor must be compact and have low power consumption. Combining these constraints led to the selection of recently developed blue GaN LEDs as the light source.

Several experiments with different dyes and epoxies yielded a satisfactory combination of Coumarin 6 laser dye with an epoxy used in the manufacturing of fiberglass[2] products. The performance of this combination can be seen in Fig. 2 which depicts the measured LED output as well as the measured absorption and emission curve for Coumarin 6 in the selected epoxy. It should be noted that the use of epoxy as the solvent affected the dye by slightly red shifting and widening the absorption curve, while slightly blue shifting the emission curve. However the efficiency of the dye was not changed significantly and decreased from 85% to 80% for a concentration of 10% by mass. Using this efficiency, and overlaying the LED spectrum upon the absorption curve allows us to conclude that 45% of the energy incident upon the epoxy will be re-emitted in a spread dictated by the emission curve.

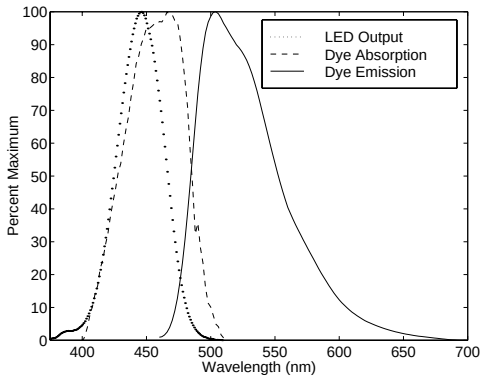

Figure 2: Characteristic curves of Coumarin 6 in epoxy solvent and light source.

The contrast between the epoxy and platen teeth is improved by filtering out reflected LED light by use of a 500 nm colored glass cut-off filter. Through analysis of the pass characteristics of the filter and the emission spectrum of the LED it is determined that 5% of this reflected light is allowed to pass through the filter. In addition, by comparing the curves in Fig. 2 one can calculate that the filter eliminates 12% of the light emitted by the dye in the epoxy. The resulting increase in contrast is clearly visible in Fig. 3, where surface features (specularities from scratches and other surface defects) can be seen in a platen illuminated with a red LED, Fig. 3*a*. However the same platen illuminated with the blue LED and filtered with the same cut-off filter, Fig. 3*b*, has most of the reflected light eliminated and what remains is light emitted by the dye in the epoxy. Surface irregularities are a significant limitation on the performance of previously reported optical sensors [6]. By using fluorescence, the only variation of signal comes in the form of varying dye concentrations, seen in Fig. 3*b* as brighter regions. These bright regions are a result of incomplete mixing of the dye in the epoxy. With proper care and mixing techniques it is felt these regions can be eliminated.

The photomicrographs in Fig. 3 were taken of a platen coated with a pigmented epoxy dye mixture.

[2] Fibreglast 10/10

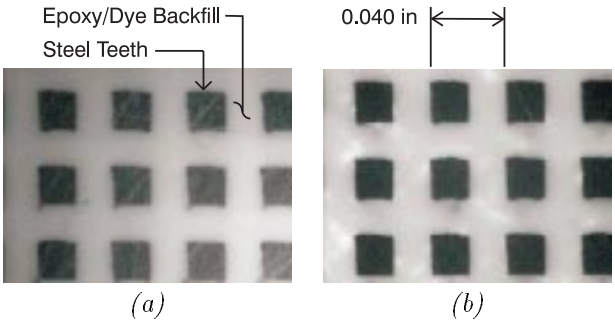

Figure 3: Photomicrograph of platen surface showing platen illuminated with *(a)* red LED with cut-off filter *(b)* blue LED with cut-off filter. Note, images are not directly comparable due to illumination differences.

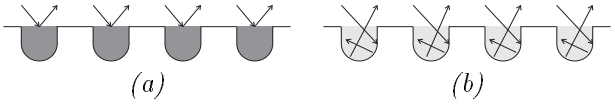

Figure 4: Diagram depicting light paths for both a platen coated with *(a)* a pigmented epoxy and *(b)* a clear epoxy.

Such a mixture produces an emitted light energy which is proportional to the surface area of epoxy visible, see Fig. 4*a*. In addition to coating this platen another platen was coated with a clear epoxy dye mixture. The rational behind such a technique is to produce a volumetric response as depicted in Fig. 4*b*.

4 Physical Design

The physical design of the sensor is composed of eight identical subsections and a mask. Each of these subsections is configured according to Fig. 5 with two illuminating LEDs and one photo-diode as a sensing element. The ends of each LED are ground off and polished, creating an effective point light source. In addition each LED is recessed into a reflective screening fixture and aimed at a point directly below the center of the sensing element on the plane of the platen. The net effect is a fairly uniform illumination of a rectangular footprint the same size of the sensor element. The interior of each section is mirrored with reflective mylar to reduce the light energy lost on these surfaces. This sensor configuration differs with other optical approaches [7, 6] in that two illuminators and one sensing element are utilized and the illuminators are not oriented normal to the platen surface. Using two illuminators increases the overall signal by allowing more excitation. Angling the illuminators further increases the illumination intensity and has the additional effect of reducing the sensitivity of the sensor to specular return, thus minimizing the influence of the poorly controlled surface properties mentioned in Section 3.

The eight subsections are paired up, matching the

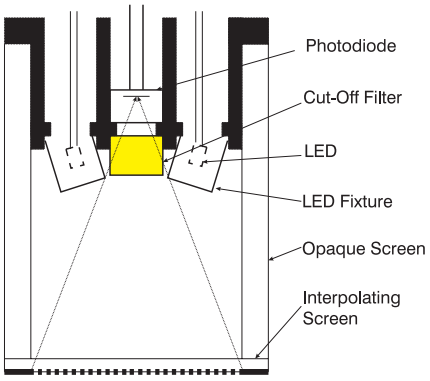

Figure 5: Schematic of sensor subsection.

shorter ends, and aligned to form a square. These subsections match the windows in the mask and are referred to as S1 - S8. They are are optically isolated from one another by opaque screens. This arrangement produces 4 quadrature pairs, two in the X direction (S1, S2, and S5, S6) and two in the Y direction (S3, S4, and S7, S8) allowing direct measurements of position in both axis as well as small rotations.

5 Electronic Design

There are many factors which cause losses of light energy within the sensor which are outlined in Section 6. For this reason the current produced by the photodiode used to measure the returned light energy is roughly 20 nA and must be converted into a voltage and amplified so that the signal can be resolved by an analog to digital converter.

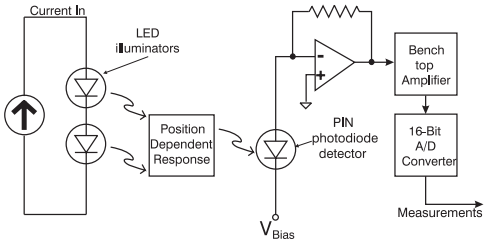

Figure 6: Electronic design of optical sensor

The design, shown in Fig. 6, begins with a current entering each of the LEDs used as illuminators. The light produced by the LEDs interact with the platen surface, dependent on the relative position of the sensor, resulting in light striking the photo-diode. The photo-diode operates in photo-conductive mode, reverse biased by 3.6 Volts and connects to a current-to-voltage converter that has a gain of 10^6. The output of this circuit is then amplified by a bench top amplifier which has an adjustable gain ranging from 10^2 to 10^3. This final signal is recorded by a 16 bit A/D converter at 100 Hz under computer control.

6 Modeling

The optical model is summarized in Fig. 7 and begins with the two LEDs producing 6 mW of light energy. A view factor loss (95%) results in 0.3 mW of light incident on the top surface of the interpolating mask. This follows from modeling the LED as a point source and considering the sensor geometry, assuming the walls have a reflective efficiency of 60%. The next loss (90%) is between the top and bottom of the interpolating mask — this represents the transparent percentage of the mask exposed. After exiting the mask, 0.03 mW of light passes through the 12 μm thick sheet of mylar which simulates the air bearing height, 10% of the signal is lost during this transition resulting in 27 μW of light energy reaching the platen. The next loss (55%) is a result of dye efficiency and the mismatch between the LED and the dye, outlined in Section 3. This results in a maximum energy output of 12 μW. The transmission back through the mylar sheet again has a loss of 10% and the 11 μW of emitted light from the dye is modeled as several point sources, originating from the windows in the interpolating mask. The view factor between the filter and the exposed dye yields a loss of 99%. Of the 0.11 μW of energy, the filter eliminates 20% due to the output spectrum of the dye and pass characteristics of the filter. The final loss (50%) is due to the efficiency of the photo-diode at the wavelengths of light detected. Thus the 87 nW are converted into 43.5 nA, which is the expected maximum output from the photo-diode, with the minimum being 22 nA.

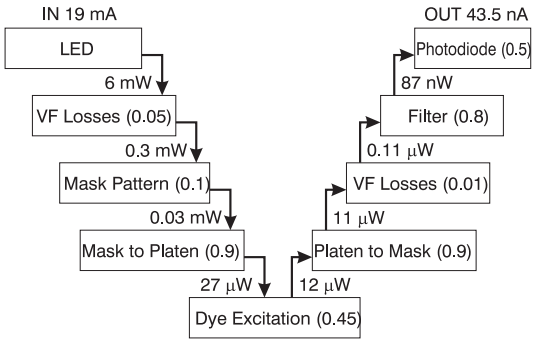

Figure 7: Model for flow of optical energy in sensor.

The combination of this model with the electronic design yields an expected peak to peak output of 22 V. The dominant losses are in the view factors which are considered to be worst case with a conservative model for both the reflectance and light source models. However there are some effects that are left unmodeled in this analysis. The most significant feature not included in the model is the transmission of light through the opaque area in the interpolating mask. The effect of this would be a reduction of the peak-to-peak signal, which could be significant due to the fact that 90% of the lit sensor footprint is opaque, and only 10% is used for sensing.

7 Results

The results discussed were obtained by maintaining the sensor stationary and moving a 30 $\times$ 30 cm test platen underneath it. Motion control of the platen section was performed with a two axis NEAT microstepping stage[3]. These results represent data collected from two quadrature pairs (S1,S2 and S5,S6), oriented along the same axis. Quadrature pair S1, S2 was outfitted with red LEDs and quadrature pair S5, S6 was outfitted with blue LEDs. The pair outfitted with the red LEDs sensed a signal associated with the platen's reflectance, while that of the blue sensed a signal created by the dye emission. Both pairs had identical geometric configurations and care was taken so that all LEDs produced the same optical power.

During experimentation, measurements were taken at 10 μm intervals with each measurements sampled 200 times at 100 Hz. The resulting mean and standard deviation were recorded and used to determine the resolution of the sensor.

7.1 Reflective Sensor Performance

The signal produced by the sensor sections outfitted with the red LEDs was the inverse of all other published reflectance based sensors — maximum reflection when the epoxy is exposed. This is a result of the geometry of the sensor not being optimized to detect specular reflection, and the backfill being a high quality lambertian surface. This observation is even further supported by the photomicrograph in Fig. 3*a* where one can easily see the higher return of the epoxy surface.

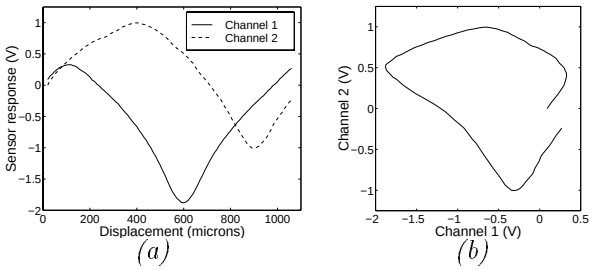

Figure 8: Data collected using reflectance technique *(a)* Channels one and two output and *(b)* quadrature relationship.

Fig. 8*a* depics and unexpected result, the output signals do not follow the predicted sharp sawtooth

[3]NEAT positioning table by New England Affiliated Technologies, Inc.

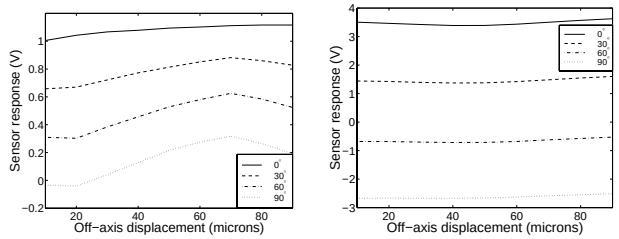

Figure 9: Off-axis motion of sensor along platen showing variation of the different phases of the *(a)* reflectance technique and the *(b)* fluorescence technique.

modulation, but rather have curved peaks and valleys. The most likely explanation of this result is that the gap between the platen and the interpolating mask is "dulling" the sharpness of the teeth. Adding to this dulling effect are angular misalignments between the mask slits and platen.

The effects of variable surface reflection on this reflectance-based sensor can be seen in Fig. 8*b* and Fig. 9*a* which coincide to quadrature and off-axis motion experiments respectively. These figures demonstrate the unpredictable variation in the sensed reflectance from one tooth to the next. In addition, motion in the direction parallel to the slits in the mask (off-axis) clearly causes variation in both the peak-to-peak and offset of the signal. Though the signal to noise ratio is approximately 1000 (1σ), see Fig. 10, the ability to use this sensor for interpolation is severely limited by the unmodeled spatial noise.

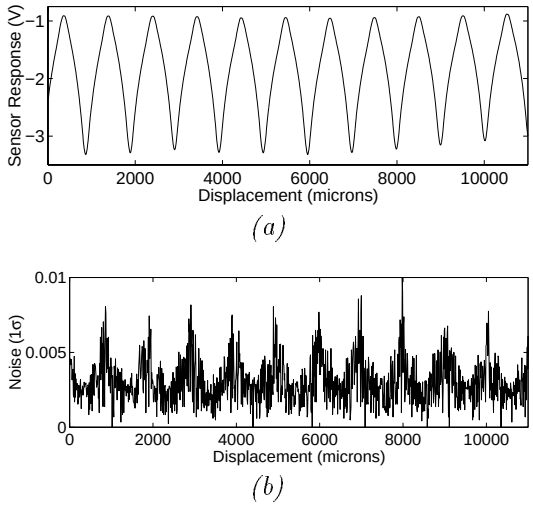

Figure 10: Reflectance sensor results for a test over 10 adjacent pitches showing *(a)* the trace of the sensor response and *(b)* the 1σ noise associated with each position.

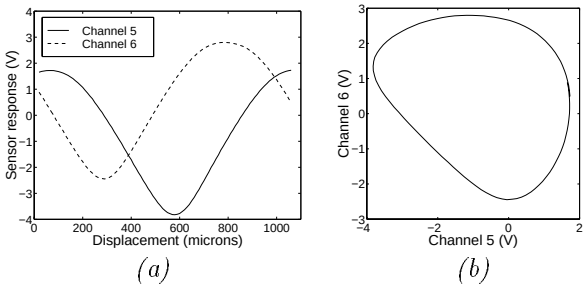

Figure 11: Data collected using fluorescence technique *(a)* Channels five and six output and *(b)* quadrature relationship.

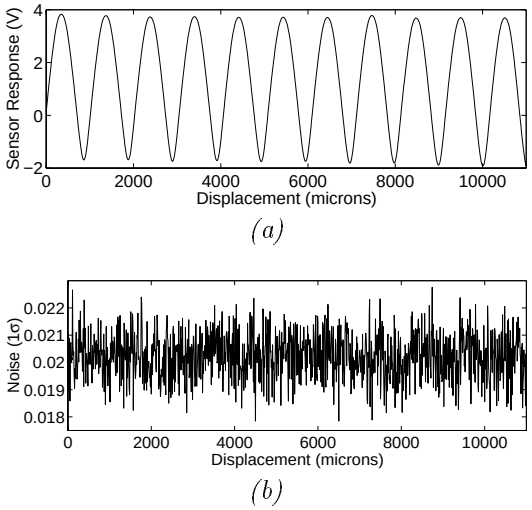

Figure 12: Fluorescence sensor results for a test over 10 adjacent pitches showing *(a)* the trace of the sensor response and *(b)* the 1σ noise associated with each position.

7.2 Fluorescent Sensor Performance

The signal produced by the sensor section outfitted with the blue LEDs also has the curved peaks and valleys. The explanation for this unpredicted result is the same as that for the reflectance technique because both configurations have identical geometry. However optically they are quite different, and this feature is visible in the reduced sensitivity of the fluorescence technique to surface features. This can be seen in the quadrature relationship, Fig. 11*(b)*, which is reproducible across the platen.

The reproducibility of this technique is accentuated by Fig. 11*a* in the fact that Channels 5 and 6 have peak to peak signals within 5 percent of each other, and maintain their respective signals within 2 percent along the platen, as seen in Fig. 9*b*.

The low variation can also be seen in Fig. 12*a* which is a trace of the modulation over several adjacent teeth.

Comparing this to the plot created by the reflectance technique over the same platen section, one can see the positive effect which the fluorescent technique provides. However the signal to noise ratio of this configuration is one third less, 330 (1σ), due to lower signal levels and increased amplification of electronic noise, Fig. 12*b*. Such a ratio yields a sensor resolution of 1 μm. A majority of the remaining noise results from electronic pickup in our experiments and can be significantly reduced by better electronic design. Furthermore, increasing the overall signal with a better optical configuration will also improve performance. Such a change could easily accomplished by increasing the incident light until the dye is quenched. In the experiments reported here the dye was less than half quenched.

7.3 Use of Clear Epoxy

The rational behind using a clear epoxy was to increase the potential light energy emitted by the dye in the epoxy by exciting a volume. However, the signal produced by the fluorescence technique across one pitch turns out to be bimodal, see Fig. 13*b*. We believe this is due to incident light exciting dye molecules not within the boundaries created by the slit in the interpolating mask. Since the epoxy is clear, incident photons are able to excite a limited region underneath the mask. Thus the second, smaller peak, occurs when the slit is aligned with the platen teeth, and the original peak when the slit is aligned with the epoxy-filled grooves.

Surprisingly, the use of a clear epoxy fill increased the signal of the reflectance technique, even though the clear fill was less reflective that the opaque one, see Fig. 13*a*. The cause for the doubling of the signal is probably due to reflected light being focussed by the curvature at the bottom of the grooves in the platen. However the spatial noise was the same with signal variation reaching up to 20 percent.

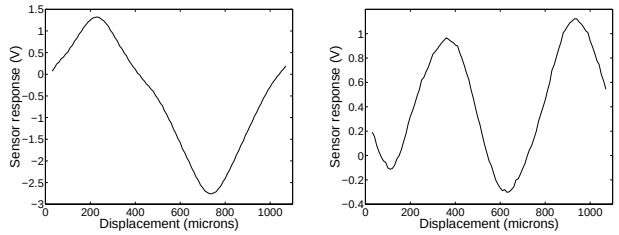

(a) *(b)*

Figure 13: Sensor response of platen coated with dye impregnated clear epoxy *(a)* of the reflectance technique and *(b)* the fluorescence technique.

8 Conclusion

The use of a fluorescence technique produces a sensor that is nearly immune to surface defects which have limited the performance of previous optical sensors. It has been shown that for identical sensor configurations a fluorescence technique with a homogeneous epoxy dye mixture has significantly less spatial noise than that of a reflectance technique. The major disadvantage of using such a technique is an overall reduction of signal. For these reasons one must pay close attention to the key losses in the optical model of the sensor. In order to reduce losses in view factors a new configuration should have a larger sensing element which is closer to the interpolating mask. In addition the number of slits on the mask should be reduced and the LEDs should be focussed onto it with a lens.

Acknowledgments

The work presented in this paper was supported in part by the NSF under grant DMI-9523156. The optical spectrum measurements were performed at the Mellon Institute under the guidance of Dr. Ratnakar Mujumdar.

References

[1] E. R. Pelta, "Two-axis Sawyer motor for motion systems" in *IEEE Control Systems magazine*, pp. 20-24, October, 1987.

[2] A. A. Rizzi, J. Gowdy, and R. L. Hollis, "Agile Assembly Architecture: An Agent-Based Approach to Modular Precision Assembly Systems" in *Proc. Int'l Conf. on Robotics and Automation*, pp. 1511-1516, April, 1997.

[3] G. L. Miller "Capacitively incremental position measurement and motion control" U.S. Patent 4,893,071, January 9 1990.

[4] J. Ish-Shalom, "Modeling of Sawyer Planar Sensor and Motor Dependence on Planar Yaw Angle Rotation" in *Proc. Int'l Conf. on Robotics and Automation*, pp. 3499-3504, April, 1997.

[5] Z. J. Butler, A. A. Rizzi, and R. L. Hollis, "Integrated Precision 3-DOF Position Sensor for Planar Linear Motors" in *Proc. Int'l Conf. on Robotics and Automation*, pp. 2652-2658, May, 1998.

[6] E. J. Nicolson and et al., "Optical sensing for closed-loop control of linear stepper motors" in *Proc. Int'l Conf. on Advanced Mechatronics*, (Tokyo, Japan), August, 1993.

[7] A. E. Brennemann and R. L. Hollis, "Magnetic and Optical-Fluorescence Position Sensing for Planar Linear Motors" in *Proc. Int'l Conf. on Intelligent Robots and Systems*, vol. 3, pp. 101-107, August, 1995.

[8] A. E. Quaid and R. L. Hollis, "3-DOF Closed-loop Control for Planar Linear Motors" in *Proc. Int'l Conf. on Robotics and Automation*, pp. 2488-2493, May, 1998.

[9] D. Crawford, F. Y. Wong, and K. Youcef-Toumi, "Modeling and Design of a Sensor for Two Dimensional Linear Motors" in *Proc. Int'l Conf. on Robotics and Automation*, pp. 2367-2372, May, 1995.